Robust inter-beat interval estimation in cardiac vibration signals

2013 Physiol. Meas. 34 123

(http://iopscience.iop.org/0967-3334/34/2/123)

IOP PUBLISHING PHYSIOLOGICAL MEASUREMENT

Physiol. Meas. **34** (2013) 123–138 doi:10.1088/0967-3334/34/2/123

Robust inter-beat interval estimation in cardiac vibration signals

C Brüser[1], **S Winter**[2] **and S Leonhardt**[1]

[1] Philips Chair of Medical Information Technology, Helmholtz-Institute for Biomedical Engineering, RWTH Aachen University, Aachen, Germany
[2] Philips Technologie GmbH Innovative Technologies, Research Laboratories, Aachen, Germany

E-mail: brueser@hia.rwth-aachen.de

Received 23 October 2012, accepted for publication 18 December 2012
Published 23 January 2013
Online at stacks.iop.org/PM/34/123

Abstract
Reliable and accurate estimation of instantaneous frequencies of physiological rhythms, such as heart rate, is critical for many healthcare applications. Robust estimation is especially challenging when novel unobtrusive sensors are used for continuous health monitoring in uncontrolled environments, because these sensors can create significant amounts of potentially unreliable data. We propose a new flexible algorithm for the robust estimation of local (beat-to-beat) intervals from cardiac vibration signals, specifically ballistocardiograms (BCGs), recorded by an unobtrusive bed-mounted sensor. This sensor allows the measurement of motions of the body which are caused by cardiac activity. Our method requires neither a training phase nor any prior knowledge about the morphology of the heart beats in the analyzed waveforms. Instead, three short-time estimators are combined using a Bayesian approach to continuously estimate the inter-beat intervals. We have validated our method on over-night BCG recordings from 33 subjects (8 normal, 25 insomniacs). On this dataset, containing approximately one million heart beats, our method achieved a mean beat-to-beat interval error of 0.78% with a coverage of 72.69%.

Keywords: ballistocardiogram, beat-to-beat heart rate, instantaneous heart rate

(Some figures may appear in colour only in the online journal)

1. Introduction

Accurate knowledge of physiological rhythms, such as heart rate, is of crucial importance in many health care applications including diagnosis, patient monitoring and treatment. Accordingly, the estimation of the time-varying frequencies of these rhythms from

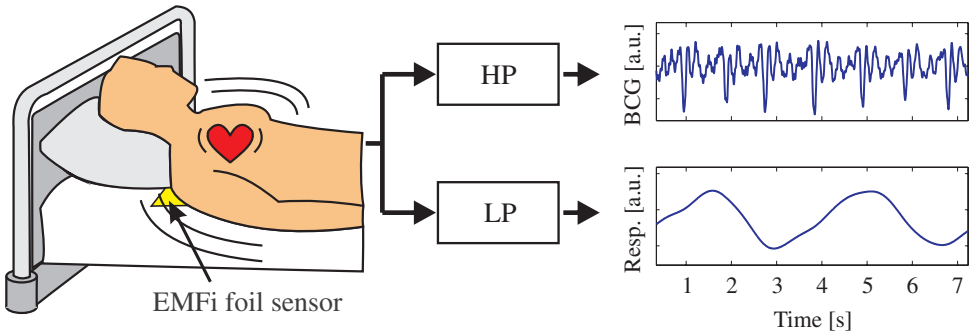

Figure 1. BCG measurement system overview. The EMFi signal is low-pass (LP) and high-pass (HP) filtered to extract its BCG and respiratory components.

conventional clinical measurement modalities such as electrocardiography (ECG) is a well-studied problem (Köhler *et al* 2002). While for some applications, it might be sufficient to estimate only an average frequency over multiple periods of the underlying rhythm, others, such as heart rate variability (HRV) analysis (Task Force of The European Society of Cardiology and The North American Society of Pacing and Electrophysiology 1996), require a beat-to-beat resolution.

Due to demographic changes and growing numbers of patients with chronic conditions, home monitoring of a patient's health status will play a pivotal role in future healthcare systems. Recent studies have shown that home telehealth approaches can lead to a significant reduction of hospital admissions and numbers of bed days of care (Darkins *et al* 2008).

Since conventional measurement modalities are often difficult to use outside clinical settings, unobtrusive and unconstrained measurement systems are currently emerging as a way to allow continuous long-term monitoring of a patient's health status (Lim *et al* 2011). These systems aim to provide two advantages over current approaches: they usually require no user interaction nor compliance to perform their measurements and they do not interfere with the user's daily routine. One family of systems, which has gained increased interest lately, are cardiac and respiratory vibration signals recorded by sensors embedded into objects of daily living (Inan 2012). Such ballistocardiogram (BCG) or seismocardiogram (SCG) sensors have been integrated into beds (Brüser *et al* 2011, Kortelainen *et al* 2010, Watanabe *et al* 2005, Paalasmaa 2010, Mack *et al* 2009), chairs (Junnila *et al* 2008), weighing scales (Inan *et al* 2012), wearable vests (Rienzo *et al* 2011) or ear-mounted devices (He *et al* 2012). While these systems offer the aforementioned advantages over established clinical methods, they also come with their own set of drawbacks. Most notably, the signal quality can be highly varying and unreliable due to the often uncontrolled environment in which the measurements are performed. For bed-mounted sensors in particular, the morphology of the recorded signals can change drastically depending on the orientation and position of the user with respect to the sensor (Brüser *et al* 2011). As we will explain in the following, reliable estimation of beat-to-beat intervals can pose significant challenges under these circumstances. It should also be noted that these methods record the mechanical activity of the heart as opposed to the ECG which records its electrical excitation. This can lead to some inherent differences in terms of beat-to-beat timings between these methods.

Figure 1 shows a schematic of a bed-based system which uses an electro-mechanical film (EMFi) sensor to record cardiac and respiratory movements. In Tavakolian and Ngai (2009),

the authors show that EMFi sensor signals contain both a BCG component caused by the aortic circulation of the blood as well as an SCG component caused by myocardial vibrations. While we acknowledge these findings and naming conventions, we will, for the sake of brevity, refer to our recorded signals as BCGs.

A typical approach for computing beat-to-beat intervals in biomedical signal processing consists of first locating the relevant events of interest, such as the QRS complex in the ECG, and then differencing successive occurrence times of these events to obtain beat-to-beat intervals. The detection of the respective events is typically based on some prior knowledge about the basic characteristic features of the event. For instance, in the case of the ECG, it is known *a priori* that a typical heart beat consists of the PQRST waves. While the exact timing, polarity, amplitude and shape of these waves can differ depending on the recorded lead and the patient's physiology, the basic morphology always follows a similar pattern. Hence, signal delineation usually starts with the detection of the QRS complex, knowing that it presents the most prominent deflection in a typical ECG (Köhler *et al* 2002, Hamilton and Tompkins 1986, Martínez *et al* 2004).

As explained before, in the case of bed-mounted BCG-based systems, on the other hand, we do not have the same type of prior knowledge about the signal. The heart beat morphology shows strong inter- and intra-subject variability (Brüser *et al* 2011). To overcome this problem, we have previously suggested using a clustering method to automatically determine a suitable heart beat template for any given BCG recording (Brüser *et al* 2011). Based on this template, subsequent heart beats can then be localized. While we could achieve promising results with this approach, it possesses one important weak point: it is heavily dependent on a successful training phase. If the algorithm learned the wrong pattern during the unsupervised training, all subsequent heart beat detection attempts will fail. Furthermore, training has to be re-initiated whenever the heart beat templates varies, for example due to posture changes. Hence, reliably determining the location of individual heart beats in BCGs remains challenging. Other groups have often applied conceptually similar approaches, where either some form of template is learned (Rosales *et al* 2012, Paalasmaa and Ranta 2008) or a specific fiducial point is located (Choi *et al* 2009). As an exception, the authors of Kortelainen *et al* (2010) suggest Fourier-domain averaging of multiple BCG channels together with a cepstrum analysis to estimate inter-beat-intervals.

In fact, for many applications, we are not even directly interested in the exact locations of individual heart beats. Instead, what we ultimately want to determine are the corresponding beat-to-beat intervals. Therefore, we propose to estimate these quantities directly from the signal without explicitly detecting particular events first. This allows us to largely avoid the problems associated with the unknown morphology of the BCG signal. Accordingly, we present a novel robust algorithm for the direct estimation of these interval lengths which does not require any prior knowledge about the morphology of the analyzed signal, yet allows beat-to-beat heart rates to be accurately extracted.

2. Continuous local interval estimation

The following algorithm provides a framework for the estimation of local (beat-to-beat) interval lengths from BCGs. Given a BCG signal $x(t)$, let $t_k,\ k \in \{1, \ldots, N\}$, denote the times at which heart beats occur in $x(t)$. We can then define the local interval lengths as well as the local frequency as

$$T_k = t_k - t_{k-1} \tag{1}$$

and

$$f_k = \frac{1}{T_k}, \tag{2}$$

respectively.

Unlike many existing methods, we do not start by detecting the location of individual events, i.e. t_k, in order to determine the corresponding interval lengths T_k. Instead, we aim to directly estimate T_k from the fundamental frequencies of the signal. This approach is inspired by what is commonly known as pitch tracking in the speech processing community (Rabiner 1977, Ross *et al* 1974, Shimamura and Kobayashi 2001). Pitch tracking refers to the estimation of the varying fundamental frequency of voiced speech segments. For our application, we consider the fundamental frequency we want to track to be the event-to-event frequency f_k as defined in (2).

A common approach to pitch tracking uses some estimator of the fundamental frequency, such as the signal's autocorrelation, on a moving analysis window. This is a mature and successful approach in speech processing. Hence, we propose to apply a similar concept for the estimation of beat-to-beat interval lengths. Nonetheless, for our application, we have to consider one important difference. In speech processing, the window size is typically chosen to contain multiple oscillations of the fundamental frequency, while at the same time, being short enough with respect to the expected rate of change of the frequency over time. However, since we aim to estimate frequency changes with an event-to-event resolution, our analysis window should ideally contain only two heart beats. To compensate the short window length, we propose to combine three estimators to improve the robustness for the fundamental frequency estimation in each window.

To summarize, local periodicity is estimated using a short analysis window (ideally containing two events of interest). This window is shifted across the signal using increments that are short with respect to the expected interval lengths, thus causing each interval to appear in multiple consecutive analysis windows. Our method gains its robustness by exploiting this redundancy as well as by combining three methods to estimate the periodicity in each analysis window.

2.1. Pre-processing

Let $x_{\mathrm{raw}}[n]$ denote the raw digital sensor signal with a sampling frequency of f_s. First, x_{raw} was pre-processed using a band-pass filter that is appropriate for the physiological rhythm which we want to extract from the given signal. The filtered signal is denoted as $x[n]$. To extract the cardiac components of the BCG, we applied an equiripple finite impulse response (FIR) filter with stop-band frequencies of 0.5 and 20 Hz. The first derivative of the filtered signals, computed using a Savitzky–Golay filter, was then used for the analysis since it enhances the transient characteristics of the BCG waveform, such as the sometimes steep flanks coinciding with the ejection of blood from the ventricles. In any case, the filter should be designed such that the base frequencies as well as the higher-order harmonics of the rhythm under analysis are located in the passband of the respective filter.

2.2. Basic algorithm

The proposed method iteratively shifts a short analysis window across the signal. During each iteration, the local interval length T_i in the analysis window is estimated. In order to improve the robustness of the estimation, the admissible values of T_i are constrained by two thresholds T_{min} and T_{max}. These thresholds are selected based on prior knowledge about the expected

range of heart rates (40–140 bpm). While the upper limit might appear low, we believe it is sufficient since we are dealing with subjects who are lying in bed at rest. The following steps comprise the ith iteration of the algorithm.

(i) Extract analysis window $w_i[\nu]$ centered at sample n_i. The window size is chosen to be twice the maximum interval length in order to ensure that it will contain at least two complete events.

$$w_i[\nu] = x[n_i + \nu], \quad \nu \in \{-T_{\max} \cdot f_s, \ldots, T_{\max} \cdot f_s\} \tag{3}$$

(ii) Compute maximum amplitude range r_i of the analysis window and check if r_i lies within specific thresholds. Since motion artifacts have typically much higher amplitudes than an undistorted BCG, a valid signal in the analysis window is assumed if r_i lies within the thresholds. Otherwise, the window is marked as invalid (artifact) and the algorithm skips to step (iv).

(iii) Estimate local interval length T_i in $w_i[\nu]$ (see section 2.3 for details).

(iv) Shift the center of the analysis window for the next iteration by a constant value Δt.

$$n_{i+1} = n_i + \Delta t \cdot f_s \tag{4}$$

2.3. Interval length estimators

For each analysis window $w_i[\nu]$, the local interval length T_i is estimated. We have chosen to combine the following three estimators which are evaluated at each admissible discrete interval length $N \in \{N_{\min}, \ldots, N_{\max}\}$, with $N_{\min} = T_{\min} \cdot f_s$ and $N_{\max} = T_{\max} \cdot f_s$. For better readability, the iteration index i is omitted in the following description.

(i) *Modified autocorrelation*. Since correlation based methods (Rabiner 1977) are known to be comparatively robust against noise (Shimamura and Kobayashi 2001), we use a modified autocorrelation function as our first interval estimator. The modified autocorrelation function $S_{\text{Corr}}[N]$ of the analysis window is computed for all discrete lags, i.e. interval lengths N, which are within the search boundaries:

$$S_{\text{Corr}}[N] = \frac{1}{N} \sum_{\nu=0}^{N} w[\nu] w[\nu - N]. \tag{5}$$

This definition differs from the traditional autocorrelation. Instead of using a fixed window size, the upper limit of the sum is set to the lag N. Since $w[0]$ denotes the center of the analysis window, this means that for each lag N, the correlation between the N samples to the right and to the left of the window center (i.e. $w[\nu]$ and $w[\nu - N]$, respectively) is computed. Through these modifications, we can ensure that for each lag, only the minimum number of samples necessary to detect a single interval of this length are considered. Hence, we avoid accidentally averaging across more than one event-to-event interval. Furthermore, through our choice of limits, the window center is always also the center of the interval to be estimated. Figure 2 visualizes this approach.

(ii) *Modified average magnitude difference function (AMDF)*. The modified AMDF (Ross *et al* 1974) is similar to the autocorrelation, frequently used in pitch tracking, and described by

$$S_{\text{AMDF}}[N] = \left(\frac{1}{N} \sum_{\nu=0}^{N} |w[\nu] - w[\nu - N]| \right)^{-1}. \tag{6}$$

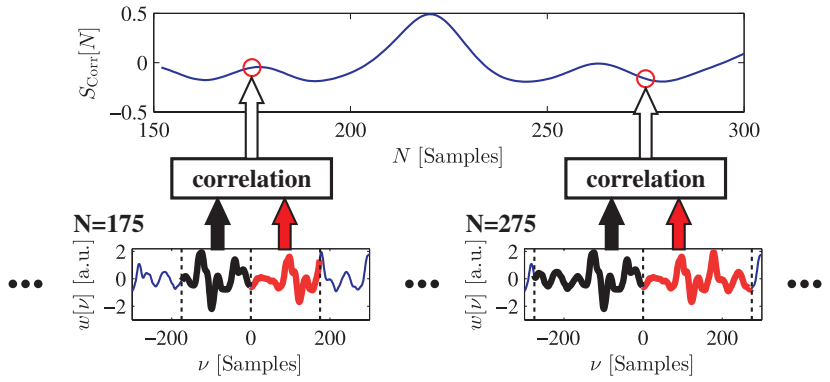

Figure 2. Working principle of the modified autocorrelation function. For each lag N, only $2N$ samples, i.e. the minimum number of samples necessary to detect a lag of N, are considered. This approach avoids the problems associated with a static autocorrelation window length, i.e. either averaging over multiple intervals (if the window is too long) or not being able to fit two events into the window (if it is chosen too short).

Note how the original AMDF takes smaller values when $w[\nu]$ and $w[\nu - N]$ become similar while the autocorrelation takes larger values. Therefore, we consider its inverse in (6), so that both estimators behave similar, i.e. take larger values for more likely interval lengths N. Furthermore, as shown in Shimamura and Kobayashi (2001), it has different noise characteristics compared to the autocorrelation, which allows the two methods to complement each other.

(iii) *Maximum amplitude pairs (MAP).* The third estimator we propose uses the amplitude information of the signal and can be considered as an indirect peak detector. It is defined as

$$S_{\mathrm{MAP}}[N] = \max_{\nu \in \{0,\ldots,N\}} (w[\nu] + w[\nu - N]). \tag{7}$$

For each possible lag N, the maximum amplitude of any pair of samples which are exactly N samples apart is determined. $S_{\mathrm{M}}[N]$ increases for values of N, if two peaks exist in the analysis window which are N samples apart.

2.4. Probabilistic estimator fusion

In order to combine the three estimators, we apply a probabilistic Bayesian interpretation of the problem. First of all, we suggest interpreting the estimator outputs of the autocorrelation (S_{Corr}), average magnitude difference function (S_{AMDF}), and maximum amplitude pairs (S_{MAP}) as posterior probability density functions $p(N|S_{\mathrm{Corr}})$, $p(N|S_{\mathrm{AMDF}})$, and $p(N|S_{\mathrm{MAP}})$, respectively. These probability density functions (PDF) shall describe the probability of N being the 'true' underlying interval length under the condition of one specific estimator. This interpretation is reasonable since each estimator behaves like a PDF in that it provides a 'probability' for how likely it is for each possible interval N to be the true interval. To obtain proper PDFs, i.e. area under the curve of one and no negative probabilities, each estimator is simply scaled linearly to satisfy these conditions. Now, given the three separate estimators, we aim to determine the most likely value of N under the combination of these three, i.e.

$$N_i = \arg\max_N \; p(N|S_{\mathrm{Corr}}, S_{\mathrm{AMDF}}, S_{\mathrm{MAP}}), \tag{8}$$

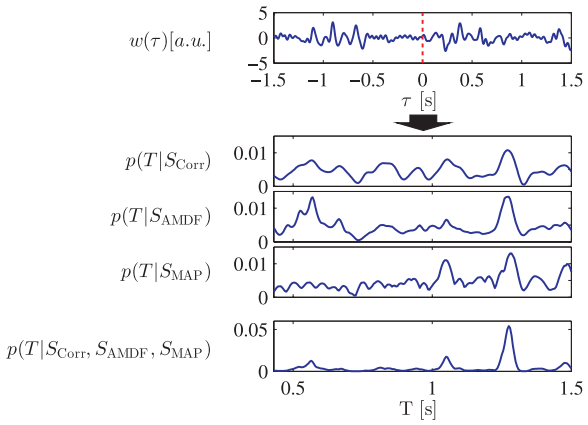

Figure 3. Example of probability density functions for each estimator derived from the analysis window $w(\tau)$: autocorrelation $p(T|S_{\mathrm{Corr}})$, AMDF $p(T|S_{\mathrm{AMDF}})$, and maximum amplitude pairs $p(T|S_{\mathrm{MAP}})$, as well as the joint estimate $p(T|S_{\mathrm{Corr}}, S_{\mathrm{AMDF}}, S_{\mathrm{MAP}})$. The combination of the indicator functions shows a clear peak at the fundamental interval length found in the analysis window. Note that the arguments were converted from samples (ν and N) to seconds (τ and T, respectively) for easier interpretation.

where $p(N|S_{\mathrm{Corr}}, S_{\mathrm{AMDF}}, S_{\mathrm{MAP}})$ denotes the conditional probability of N being the true interval length given the joint estimator outputs. According to Bayes' theorem, this posterior probability can be expressed as

$$p(N|S_{\mathrm{Corr}}, S_{\mathrm{AMDF}}, S_{\mathrm{MAP}}) = \frac{p(S_{\mathrm{Corr}}, S_{\mathrm{AMDF}}, S_{\mathrm{MAP}}|N)\, p(N)}{p(S_{\mathrm{Corr}}, S_{\mathrm{AMDF}}, S_{\mathrm{MAP}})}, \tag{9}$$

where the denominator is a constant scaling factor which does not depend on N and will thus be disregarded in the following. Under the reasonable assumption that the likelihood of each estimator only depends on the true interval length of the signal and not on the other estimators' outputs, the numerator of (9) can be rewritten, resulting in

$$p(N|S_{\mathrm{Corr}}, S_{\mathrm{AMDF}}, S_{\mathrm{MAP}}) \propto p(S_{\mathrm{Corr}}|N)\, p(S_{\mathrm{AMDF}}|N)\, p(S_{\mathrm{MAP}}|N)\, p(N). \tag{10}$$

Applying Bayes' theorem a second time to the individual likelihoods, again dropping constant factors which are independent of N, yields

$$p(N|S_{\mathrm{Corr}}, S_{\mathrm{AMDF}}, S_{\mathrm{MAP}}) \propto p(N|S_{\mathrm{Corr}})\, p(N|S_{\mathrm{AMDF}})\, p(N|S_{\mathrm{MAP}})\, p(N)^{-2}. \tag{11}$$

Since we do not want to impose any constraints on the possible interval lengths, we have chosen to use an uninformed prior $p(N)$ with a uniform distribution, which simplifies (11) to

$$p(N|S_{\mathrm{Corr}}, S_{\mathrm{AMDF}}, S_{\mathrm{MAP}}) \propto p(N|S_{\mathrm{Corr}})\, p(N|S_{\mathrm{AMDF}})\, p(N|S_{\mathrm{MAP}}). \tag{12}$$

Thus, we can obtain the most likely joint estimate of the interval length N_i for the ith analysis window, by selecting the maximum of the product of the three scaled estimator outputs according to (8). The interval length in seconds immediately follows as $T_i = N_i/f_s$.

Furthermore, the value of $p(N|S_{\mathrm{Corr}}, S_{\mathrm{AMDF}}, S_{\mathrm{MAP}})$ for the selected value $N = N_i$ can also be used as a measure of confidence in the estimation. To obtain values comparable among different analysis windows, the right-hand side of (12) simply needs to be scaled to a proper PDF, i.e. to an area under the curve of one.

Figure 3 shows an example of the individual PDFs for each estimator as well as the joint estimate. The joint PDF shows one clear peak at the beat-to-beat interval found in this

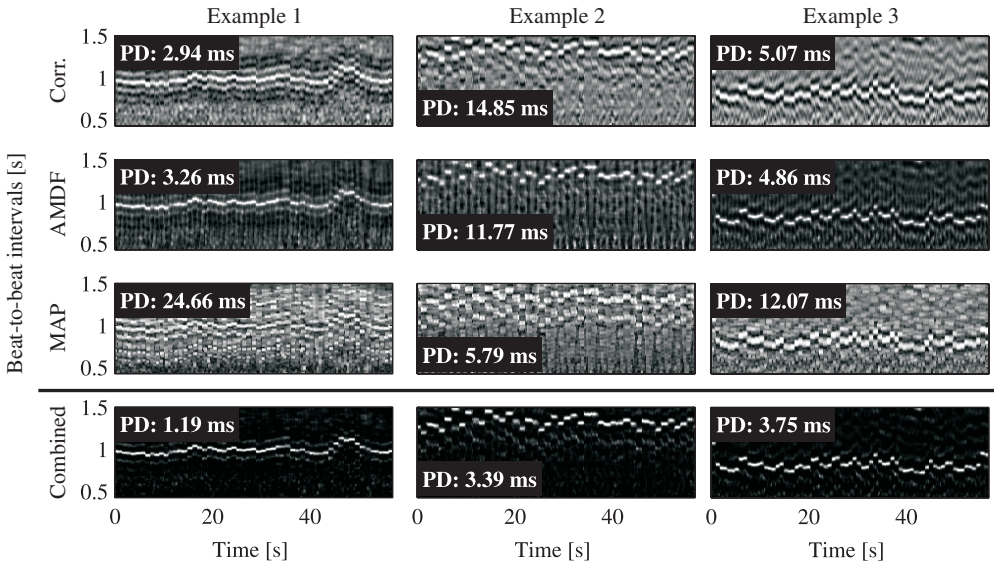

Figure 4. Two-dimensional representations of beat-to-beat interval probabilities obtained from each of the individual estimators, as well as their combination, for three sample BCGs. Each pixel shows the estimated probability for a particular interval length (*y*-axis) at a given point in time (*x*-axis). Brightness increases with probability. Peak deviation (PD) quantifies the mean absolute deviation between the intervals with the highest probability and an ECG-derived reference.

analysis window. Furthermore, three one-minute-long examples are visualized in figure 4. In all examples, the combined estimator shows a clear white line tracking the true beat-to-beat intervals. To quantify the estimators' agreements with an ECG-derived reference, the mean absolute deviation between the reference and the interval with the highest probability, at each point in time, is computed. The accuracy of the individual estimators varies among the examples, i.e. MAP has the worst accuracy in example 1, while it is the most accurate estimator in example 2. This shows that depending on the signal, the various estimators perform differently and thus complement each other. In addition, we can observe that the combined estimate is always more accurate than even the best individual estimator, which suggests that both robustness and accuracy benefit from using multiple methods.

2.5. Extended algorithm

In its basic form, the proposed algorithm produces continuous estimates for the inter-beat intervals. Hence, individual heart beat locations are not explicitly detected. However, due to the short shifts of the analysis window, each pair of heart beats appears in multiple consecutive analysis windows and thus produces multiple estimates. In the best case, these estimates of the same underlying interval should be identical and only change once the window center is shifted into the next beat-to-beat interval. This redundancy can now be exploited in order to provide more robust results by merging all estimates belonging to the same underlying interval. The main challenge here is that we do not know beforehand where any particular beat-to-beat interval begins or ends (i.e. where the heart beats are located). To this end, we introduce an extended version of the basic algorithm.

We assume that each interval is delimited by heart beats consisting of a structure of peaks (which might not be very distinct). However, since we already have a good estimate for the distance between these heart beats (i.e. T_i), we can use this information to narrow the search down to peaks which are: (a) approx. T_i seconds apart and (b) located to the left and right of the window center, respectively. We define the pair of peaks which fulfil these requirements and which have the largest combined amplitudes to be the boundary peaks of the interval. We suggest using the right boundary peak as an anchor point. Similar estimates of the same underlying interval should yield the same anchor point which can then be used to determine which estimates belong together. These estimates can then be safely merged without accidentally averaging across neighboring intervals.

Let $\mathbf{M}_i$ denote the set of peaks located in the right half of the analysis window $w_i[\nu]$. We then define the global location of the right boundary peak of the interval T_i as

$$P_i = n_i + \underset{m \in \mathbf{M}_i \,\wedge\, m < N_i}{\arg\max} \; (w_i[m] + w_i[m - N_i]). \tag{13}$$

Let $\overline{P_k}$ denote the kth unique value among all values of P_i. We can then define the set of interval estimates belonging to that value of $\overline{P_k}$ as

$$\mathbf{T}_k = \{T_i \mid P_i = \overline{P_k}\}. \tag{14}$$

The median of this set is computed to obtain a robust estimate of the local interval length

$$\overline{T_k} = \text{median}(\mathbf{T}_k). \tag{15}$$

Thus, the final output of the algorithm consists of pairs $(\overline{P_k}, \overline{T_k})$ of peak locations and corresponding interval length estimates.

Figure 5 shows the analysis windows of multiple consecutive iterations and the derived interval lengths T_i and peak locations P_i. Using the different anchor points (P_i), the estimates belonging to the different intervals can easily be grouped together as shown in the figure. It should be stressed that the anchor points are solely used to group interval estimates together. Hence, their exact location is not relevant to the final interval estimation. Figure 6 shows an example of the extended algorithm output and how the combination of multiple interval estimates compensates outliers.

Based on the confidence values for each individual estimate T_k, a quality, or confidence, indicator $\overline{Q_k}$ can be derived by averaging the individual confidence values associated with each estimate. By applying a fixed threshold th_Q to each $\overline{Q_k}$, unreliable estimates can be excluded from further analysis.

3. Performance evaluation

In this section, we analyze the performance of the proposed method on signals obtained from an unobtrusive bed-mounted BCG sensor.

The following analysis was performed using MATLAB 7.12 (The Mathworks, Natick, MA). Our implementation of the proposed algorithm is capable of processing signals on-line, requiring only a short look-ahead window of a few seconds.

3.1. Data acquisition and performance metrics

The data used in the following analysis was recorded overnight from 8 healthy volunteers (7 female, 1 male, age: 32.8 ± 13.4 years, BMI: 25.9 ± 3.7 kg m^{-2}) and 25 insomnia patients (12 female, 13 male, 47.0 ± 13.1 years, BMI: 27.1 ± 4.1 kg m^{-2}), who gave their informed written consent, at the Boston Sleep Center, Boston, MA, USA. For each volunteer, a full

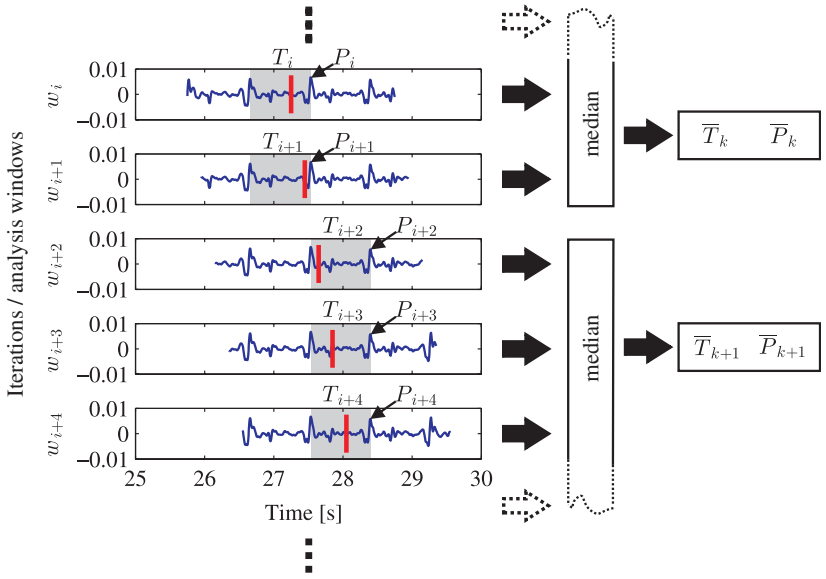

Figure 5. Analysis windows of five consecutive algorithm iterations. The same inter-beat interval (highlighted by gray shading) is analyzed in the first two iterations. This leads to identical anchor points (P_i), which can then be used to merge these interval estimates together using a median operation. In the remaining three windows, the center of the window (red vertical line) is shifted into the next inter-beat interval. Hence, the interval estimates (T_i) as well as the corresponding anchor points change, thus indicating that these estimates belong to a different underlying interval.

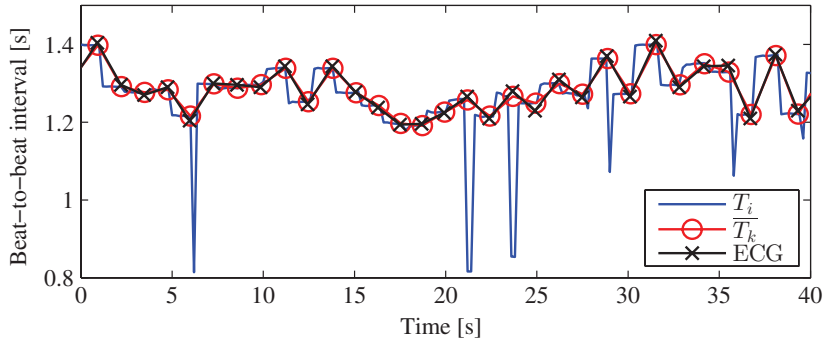

Figure 6. Output of the extended algorithm. Red circles indicate the peak locations and corresponding interval length estimates ($\overline{P}_k$, $\overline{T}_k$) computed by the algorithm. By merging individual estimates (T_i), outliers can be eliminated so that the final output correlates highly with the simultaneously recorded reference RR intervals.

polysomnograph was performed of which the lead II ECG was used in the following analysis. RR-intervals obtained by the Hamilton–Tompkins algorithm from the lead II ECGs were used as gold-standard reference (Hamilton and Tompkins 1986).

A BCG signal was acquired using a single electromechanical-film (EMFi) sensor (Emfit Ltd, Vaajakoski, Finland; dimensions: 30 cm × 60 cm , thickness < 1 mm) mounted on the underside of a thin foam overlay which was then placed on top of the mattress of a regular

bed. Figure 1 shows a schematic representation of the measurement system. Mechanical deformation of the electromechanical film generates a signal which is proportional to the dynamic force acting along the thickness direction of the sensor. The sensor was positioned where the subjects' thoraces will usually lie to record cardiac vibrations (BCG) and respiratory movements of the person lying in bed.

The performance of the proposed algorithm with respect to the estimated interval lengths has been measured by computing the following error statistics. For each estimated interval, the related interval obtained through a reference method was determined and the relative error between the two was computed. These errors were then aggregated by computing their mean ($\overline{E}$) as well as their 95th percentile (E_{95}), which describes the spread of the errors. For reference, the mean absolute error ($\overline{E}_{\text{abs}}$) is also given. Furthermore, the coverage denotes the percentage of the reference intervals for which an corresponding interval could be estimated by the proposed method.

3.2. Results

Table 1 shows the performance of the proposed algorithm on each individual recording. For the normal group, a mean error and coverage of 0.61% and 84.53%, respectively, could be achieved. The reduced coverage can be attributed to the BCG's susceptibility to motion artifacts. When the subject performs major movements in bed, the signal to noise ratio significantly decreases, making a reliable inter-beat interval estimation impossible for a few seconds. This is automatically detected by the proposed algorithm and such segments are discarded.

Compared to the normal group, the group of insomnia patients show a reduced coverage of 68.90%. The mean and especially the spread of errors (i.e. the 95th percentile of errors) is also slightly increased to 0.83% and 1.61%, respectively. We tested the statistical significance of these differences using a two-sample t-test with unpooled variances. With a significance level of $p < 0.05$, the error levels of the insomnia group are significantly increased with respect to the normal group ($p < 0.05$). The differences in coverage are also statistically significant ($p < 0.001$). Figure 7 visualizes the differences in mean errors, 95th error percentiles, and coverages between the different subjects. The higher variability of errors levels and, especially, coverages in the insomnia group is clearly visible.

The effect of the quality threshold th_Q on the coverage as well as the interval errors is shown in figure 8. We can observe that th_Q can be used to adjust the trade-off between coverage and mean errors. Higher values of th_Q exclude more estimates, thus lowering the coverage, but at the same time the average interval error of the remaining estimates is decreased. The threshold used to generate the results in this section is highlighted. We further investigated the mean of the confidence values $\bar{Q}_k$ associated with the interval estimates for each subject. Here, we found a significant correlation of $r = 0.62$ ($p < 0.001$) between the mean confidence values and the mean errors for the subjects. These results suggest that the confidence values are indeed useful to assess the quality of the resulting estimates to some degree.

Figure 9 shows a modified Bland–Altman plot of the aggregated beat-to-beat interval errors from all recordings. The plot shows a small bias of 1.4 ms in the interval errors with 90% of the errors lying between ± 10 ms. Overall, a good agreement between ECG- and BCG-derived beat-to-beat intervals can be observed.

We also processed the normal recordings with a previously published algorithm for BCG beat-to-beat interval estimation (Brüser *et al* 2011) in order to compare it to our proposed method. On the given dataset, our previous method achieved a mean coverage and interval error (95th percentile) of 86.72% and 2.56% (12.5%), respectively. These results show that our

Table 1. Beat-to-beat heart rate estimation performance of the proposed algorithm when applied to BCG signals. Errors are given as mean beat-to-beat interval error ($\overline{E}$), the corresponding 95th error percentile (E_{95}) and the mean absolute error ($\overline{E}_{\text{abs}}$).

Group	Subject	Dur. (h:mm)	Cover (%)	$\overline{E}$ (%)	E_{95} (%)	$\overline{E}_{\text{abs}}$ (ms)
	1	6:39	86.20	0.38	0.90	4.00
	2	6:45	78.45	0.53	1.23	6.29
	3	6:33	81.04	0.96	1.71	7.39
	4	6:56	87.49	0.58	1.11	5.16
	5	7:40	78.00	0.88	1.47	8.09
	6	7:30	83.32	0.63	1.40	7.54
	7	7:26	90.69	0.45	0.98	4.23
	8	6:34	91.04	0.49	1.07	3.85
Norm.	Avg.	7:00	84.53	0.61	1.23	5.82
	9	6:59	52.19	1.82	4.16	14.35
	10	7:21	71.37	0.87	1.55	7.57
	11	6:14	82.45	1.19	1.54	7.19
	12	6:32	48.09	1.17	2.46	10.06
	13	6:47	79.47	0.69	1.34	6.30
	14	6:41	60.04	0.69	1.70	8.78
	15	6:58	58.78	1.05	1.92	8.91
	16	6:37	78.58	0.64	1.13	4.85
	17	7:05	55.44	1.32	2.16	10.23
	18	6:19	40.20	1.05	1.84	12.26
	19	5:47	67.95	0.62	1.27	6.24
	20	6:21	75.56	0.65	1.26	5.02
	21	6:10	78.22	0.65	1.45	4.97
	22	7:09	54.43	1.39	2.02	13.14
	23	3:34	57.03	0.56	0.88	5.58
	24	7:43	79.18	0.61	0.96	4.88
	25	7:45	74.64	0.55	1.07	6.23
	26	4:27	34.60	1.51	3.56	14.29
	27	6:52	79.81	0.72	1.47	5.76
	28	5:44	76.09	0.57	1.30	5.87
	29	7:01	88.91	0.61	1.42	4.99
	30	7:22	86.21	0.52	1.00	4.69
	31	7:03	70.38	0.53	1.04	7.33
	32	7:16	80.89	0.46	1.00	4.64
	33	5:52	91.94	0.39	0.88	3.44
Insomn.	Avg.	6:33	68.90	0.83	1.61	7.50
Total	Avg.	6:39	72.69	0.78	1.52	7.09

new method provides significantly reduced estimation errors ($p < 0.05$) while maintaining a similar level of coverage.

4. Discussion

We evaluated our method on almost 220 h of BCG signals ($\approx$ 660.000 heart beats in the artifact-free signal segments) obtained from 33 subjects. Compared to our previous work (Brüser *et al* 2011), as well as the works of other groups in the field (Sprager and Zazula 2012, Rosales *et al* 2012), this is a fairly large data set. Not solely in terms of the number of subjects, but also with respect to the average recorded duration of approximately 6.5 h.

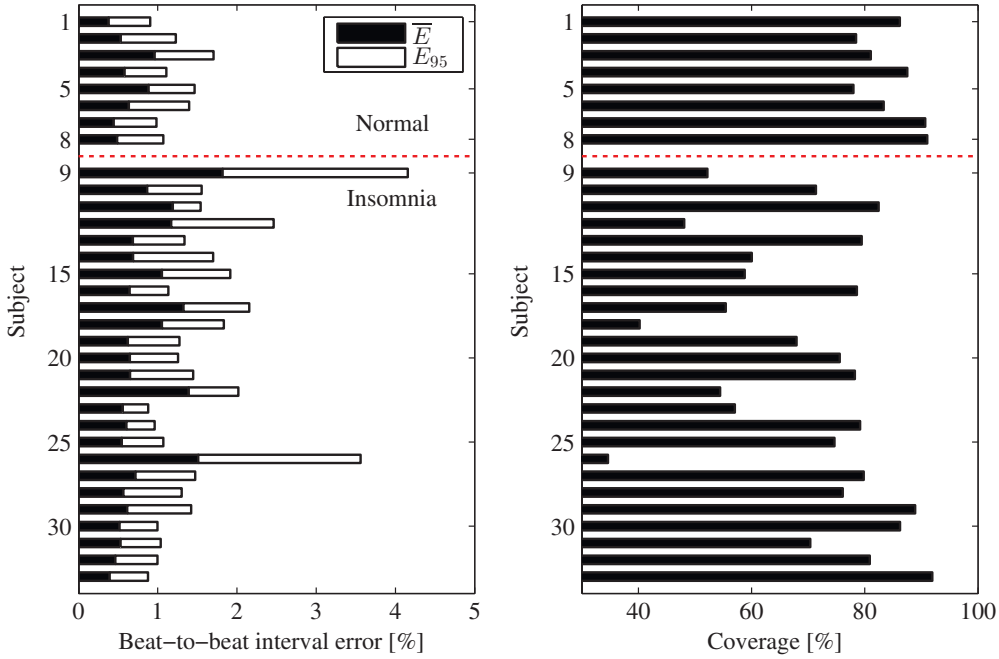

Figure 7. Bar plots showing the mean error and 95th percentile of errors as well as the coverage for each subject.

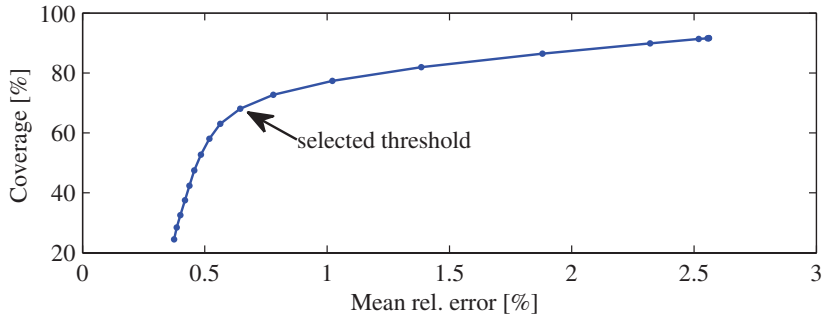

Figure 8. Coverage over mean interval error of the BCG heart rate analysis as a function of the quality threshold th_Q.

As shown in figure 9, good agreement between ECG- and BCG-derived beat-to-beat heart rates could be achieved. Among the normal subjects, the mean errors and the spread of errors were relatively consistent. In the case of the insomnia patients, however, we could observe an average increase in mean errors of 36% and a 31% increase in the errors' 95th percentiles. This means that for this group, the beat-to-beat interval estimates contained noticeably more outliers. It is important to keep in mind that the absolute error levels are still well within the lower single-digit-percentage range. A closer look at figure 7 reveals that the increased error levels in the insomnia group can be mostly attributed to two subjects with highly increased

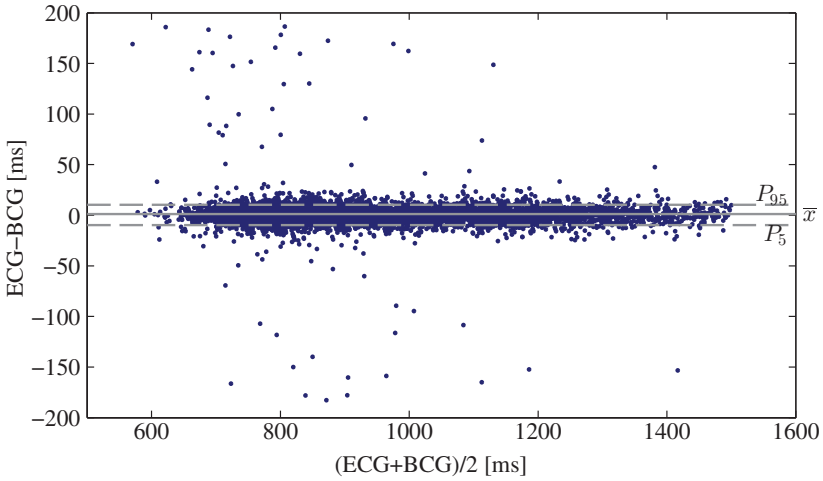

Figure 9. Bland–Altman plot of the beat-to-beat interval errors obtained from the BCG signals using the presented algorithm compared to the ECG reference intervals. To avoid clutter, 10 000 heart beats were randomly sampled from a total of 660 000 to generate this plot.

error spreads (subjects 9 and 26). For the other subjects, our algorithm was apparently capable of keeping the errors within very acceptable limits.

Intuitively, the decreased performance for the insomnia group was to be expected, which was also the very reason to include these patients in our analysis. Insomnia patients have, per definition, difficulties with falling or staying asleep. In our dataset, mean sleep efficiency for normal and insomnia subjects was 91.8% ± 4.0% and 67.9% ± 22.7%, respectively. Sleep efficiency measures the ratio of time asleep to the total time spend in bed. Due to their increased number of wakeful episodes, insomnia patients can be expected to show increased movement activity throughout the night. As discussed earlier, body motions have a major impact on the BCG signals, distorting or even destroying the signals completely. They, therefore, present a more challenging target for the measurement system as well as the proposed algorithm than the normal subjects. The higher levels of activity could, therefore, explain the decreased coverage and the slightly increased errors. These results also indicate that our proposed method is capable of maintaining low error levels, at the expense of reduced coverage, even in the presence of difficult artifact and noise conditions. We consider this to be a useful property, since we believe reliable estimates are of utmost importance to any automated monitoring system.

The main limitation of our proposed algorithm lies in the implicit assumption that two consecutive heart beats in the BCG have an unknown but similar morphology. Our results indicate that this assumption holds in general and that the obtained beat-to-beat interval will likely be suitable for estimating heart rate variability, for instance. However, at least one effect might lead to BCG signals where two consecutive heart beats are no longer similar in morphology. If an irregular heart beat with a very low stroke volume rapidly follows a regular heart beat, the second heart beat's BCG amplitude might be so small compared to the previous heart beat's that it effectively gets 'buried' in the impulse response of the former. In such a case, which can, for example, occur in some atrial fibrillation patients, the second heart beat will likely go undetected. At the same time, this might also be considered as a limitation of the BCG measurement principle in general, rather than a limitation of our proposed method

in particular. In this context, we would like to emphasize that the BCG signals analyzed in this study, unlike the ECG reference, measure mechanical cardiac activity. This means that some deviation from the ECG reference will naturally occur because two different quantities (mechanical versus electrical) are compared. In the presence of cardiac alternans, which we did not observe in our data, these differences might be significant and could affect the agreement between ECG and BCG-derived beat-to-beat heart rates.

At this point, it should also be noted that our method is highly agnostic of the actual signal it is applied to. While we developed and evaluated it for the use with BCG signals, it should be equally applicable to other cardiac, or maybe even respiratory, signals in which consecutive heart beats, or breaths, appear as similar waveforms. To the best of our knowledge, this property should apply to almost all cardiac signals typically used.

5. Conclusion

We presented a flexible online-capable algorithm for the estimation of beat-to-beat heart rates from BCG signals by means of continuous local interval estimation. The proposed algorithm combines three estimators to obtain robust interval estimates from a moving, short-time analysis window. Based on an evaluation data set of 33 overnight sleep-lab recordings, the algorithm's performance was compared to beat-to-beat heart rates obtained from a reference ECG. Analyzing signals from an unobtrusive bed-mounted BCG sensor, the proposed method achieved a mean beat-to-beat heart rate interval error of 0.78% with a mean coverage of 72.69%.

Acknowledgments

The authors thank all the colleagues from the Sleep Health Center, Boston, MA, USA, for their contribution (L Hueser, D Clarke), and particularly D White, MD for supporting this study. We also thank the anonymous reviewers for their helpful comments and suggestions.

References

Brüser C, Stadlthanner K, de Waele S and Leonhardt S 2011 Adaptive beat-to-beat heart rate estimation in ballistocardiograms *IEEE Trans. Inf. Technol. Biomed.* **15** 778–86

Choi B H, Chung G S, Lee J-S, Jeong D-U and Park K S 2009 Slow-wave sleep estimation on a load-cell-installed bed: a non-constrained method *Phys. Meas.* **30** 1163–70

Darkins A, Ryan P, Kobb R, Foster L, Edmonson E, Wakefield B and Lancaster A E 2008 Care coordination/home telehealth: the systematic implementation of health informatics, home telehealth, and disease management to support the care of veteran patients with chronic conditions *Telemed. e-Health* **14** 1118–26

He D D, Winokur E S and Sodini C G 2012 An ear-worn continuous ballistocardiogram (BCG) sensor for cardiovascular monitoring *Proc. 34th Annu. Int. Conf. IEEE Engineering in Medicine and Biology Society (San Diego, CA, USA)* pp 5030–3

Hamilton P S and Tompkins W J 1986 Quantitative investigation of QRS detection rules using the MIT/BIH arrhythmia database *IEEE Trans. Biomed. Eng.* **33** 1157–65

Inan O T 2012 Recent advances in cardiovascular monitoring using ballistocardiography *Proc. 34th Annu. Int. Conf. IEEE Engineering in Medicine and Biology Society (San Diego, CA, USA)* pp 5038–41

Inan O T, Park D, Giovangrandi L and Kovacs G T A 2012 Noninvasive measurement of physiological signals on a modified home bathroom scale *IEEE Trans. Biomed. Eng.* **59** 2137–43

Junnila S, Akhbardeh A and Värri A 2008 An electromechanical film sensor based wireless ballistocardiographic chair: implementation and performance *J. Signal Process. Syst.* **57** 305–20

Köhler B-U, Henning C and Orglmeister R 2002 The principles of software QRS detection *IEEE Eng. Med. Biol. Mag.* **21** 42–57

Kortelainen J M, Mendez M O, Bianchi A M, Matteucci M and Cerutti S 2010 Sleep staging based on signals acquired through bed sensor *IEEE Trans. Inf. Technol. Biomed.* **14** 776–85

Lim Y G, Hong K H, Kim K K, Shin J H, Lee S M, Chung G S, Baek H J, Jeong D U and Park K S 2011 Monitoring physiological signals using nonintrusive sensors installed in daily life equipment *Biomed. Eng. Lett.* **1** 11–20

Mack D C, Patrie J T, Suratt P M, Felder R A and Alwan M A 2009 Development and preliminary validation of heart rate and breathing rate detection using a passive, ballistocardiography-based sleep monitoring system *IEEE Trans. Inf. Technol. Biomed.* **13** 111–20

Martínez J P, Almeida R, Olmos S, Rocha A P and Laguna P 2004 A wavelet-based ECG delineator: evaluation on standard databases *IEEE Trans. Biomed. Eng.* **51** 570–81

Paalasmaa J 2010 A respiratory latent variable model for mechanically measured heartbeats *Phys. Meas.* **31** 1331–44

Paalasmaa J and Ranta M 2008 Detecting heartbeats in the ballistocardiogram with clustering *ICML/UAI/COLT Workshop on Machine Learning for Health-Care Applications (Helsinki, Finland)* pp 1–4

Rabiner L R 1977 On the use of autocorrelation analysis for pitch detection *IEEE Trans. Acoust. Speech Signal Process.* **25** 24–33

Rienzo M D, Meriggi P, Rizzo F, Vaini E, Faini A, Merati G, Parati G and Castiglioni P 2011 A wearable system for the seismocardiogram assessment in daily life conditions *Proc. 33rd Annu. Int. Conf. IEEE Engineering in Medicine and Biology Society (Boston, MA, USA)* pp 4263–6

Rosales L, Skubic M, Heise D, Devaney M J and Schaumburg M 2012 Heartbeat detection from a hydraulic bed sensor using a clustering approach *Proc. 34th Annu. Int. Conf. IEEE Engineering in Medicine and Biology Society (San Diego, CA, USA)* pp 2383–7

Ross M J, Shaffer H L, Gohen A, Freudberg R and Manley H J 1974 Average magnitude difference function pitch extractor *IEEE Trans. Acoust. Speech Signal Process.* **22** 353–62

Shimamura T and Kobayashi H 2001 Weighted autocorrelation for pitch extraction of noisy speech *IEEE Trans. Speech Audio Process.* **9** 727–30

Sprager S and Zazula D 2012 Heartbeat and respiration detection from optical interferometric signals by using a multimethod approach *IEEE Trans. Biomed. Eng.* **59** 2922–9

Task Force of The European Society of Cardiology and The North American Society of Pacing and Electrophysiology 1996 Heart rate variability: standards of measurement, physiological interpretation, and clinical use *Eur. Heart J.* **17** 354–81

Tavakolian K and Ngai B 2009 Comparative analysis of infrasonic cardiac signals *Comput. Cardiol.* **36** 757–60

Watanabe K, Watanabe T, Watanabe H, Ando H, Ishikawa T and Kobayashi K 2005 Noninvasive measurement of heartbeat, respiration, snoring and body movements of a subject in bed via a pneumatic method *IEEE Trans. Biomed. Eng.* **52** 2100–7